Expression of the cytoplasmic NPM1 mutant (NPMc+) causes the expansion of hematopoietic cells in zebrafish

*Niccolò Bolli,[1,2] *Elspeth M. Payne,[1,3] Clemens Grabher,[1,4] Jeong-Soo Lee,[1] Adam B. Johnston,[1] Brunangelo Falini,[2] John P. Kanki,[1] and A. Thomas Look[1,5]

[1]Department of Pediatric Oncology, Dana-Farber Cancer Institute, Harvard Medical School, Boston, MA; [2]Institute of Hematology, University of Perugia, Perugia, Italy; [3]Institute of Cancer, Barts and the London School of Medicine, London, United Kingdom; [4]Karlsruhe Institute of Technology, Forschungszentrum Karlsruhe, Karlsruhe, Germany; and [5]Division of Hematology/Oncology, Department of Pediatrics, Children's Hospital, Harvard Medical School, Boston, MA

Mutations in the human nucleophosmin (*NPM1*) gene are the most frequent genetic alteration in adult acute myeloid leukemias (AMLs) and result in aberrant cytoplasmic translocation of this nucleolar phosphoprotein (NPMc+). However, underlying mechanisms leading to leukemogenesis remain unknown. To address this issue, we took advantage of the zebrafish model organism, which expresses 2 genes orthologous to human *NPM1*, referred to as *npm1a* and *npm1b*. Both genes are ubiquitously expressed, and their knockdown produces a reduction in myeloid cell numbers that is specifically rescued by *NPM1* expression. In zebrafish, wild-type human NPM1 is nucleolar while NPMc+ is cytoplasmic, as in human AML, and both interact with endogenous zebrafish Npm1a and Npm1b. Forced NPMc+ expression in zebrafish causes an increase in *pu.1*+ primitive early myeloid cells. A more marked perturbation of myelopoiesis occurs in p53$^{m/m}$ embryos expressing NPMc+, where *mpx*+ and *csf1r*+ cell numbers are also expanded. Importantly, NPMc+ expression results in increased numbers of definitive hematopoietic cells, including erythromyeloid progenitors in the posterior blood island and *c-myb/cd41*+ cells in the ventral wall of the aorta. These results are likely to be relevant to human NPMc+ AML, where the observed NPMc+ multilineage expression pattern implies transformation of a multipotent stem or progenitor cell. (*Blood*. 2010;115(16):3329-3340)

Introduction

Nucleophosmin (NPM1) is a ubiquitous multifunctional phosphoprotein, which is normally located in the nucleolus but has nucleocytoplasmic shuttling activity. Known functions of NPM1 include roles in ribosome biogenesis and control of centrosome duplication.[1] NPM1 also regulates the tumor suppressors p14^{ARF2,3} and p53,[4] and is up-regulated by cellular stresses such as DNA damage.[5] *Npm1*$^{+/-}$ heterozygous mice are viable, and show a hematologic syndrome similar to human myelodysplastic syndrome (MDS), suggesting a role of Npm1 in hematopoiesis.[6] Moreover, *Npm1*$^{+/-}$ mice show genomic instability and a greater propensity to develop hematologic malignancies, defining *Npm1* as a haploinsufficient tumor suppressor.[7] Heterozygous gain of function mutations in *NPM1* are the most frequent genetic abnormalities found in human acute myeloid leukemia (AML), occurring in 30% of all adult cases.[8] Such mutations of *NPM1* appear to be specific to AML, as they do not occur in other human cancers.[8,9] In the absence of FLT3-ITDs, mutated *NPM1* in adult AML has been associated with a better prognosis.[10] Because of its distinctive biologic and clinical features,[11] *NPM1*-mutated AML has been included as a new provisional entity in the 2008 World Health Organization (WHO) classification of human myeloid neoplasms.[12] Consequently, *NPM1* mutational analysis is now performed routinely on adults diagnosed with AML.[10,11]

NPM1 expression is normally detected primarily in the nucleolus, but when mutated it aberrantly relocates to the cytoplasm.[13]

More than 50 mutations have been described that lead to this aberrant localization, and thus the term NPM1 cytoplasmic–positive (NPMc+) has been used to define cytoplasmic mutants that are found in AML.[8] Mechanisms underlying the aberrant localization of NPMc+ have been identified,[14,15] and studies have shown that NPMc+ can function as an oncogene in vitro[16] and disrupt murine hematopoiesis;[17] however, the critical steps leading to leukemic transformation of NPMc+-expressing cells remain unknown.

The zebrafish is a powerful vertebrate disease model system. Several human and murine oncogenes involved in leukemogenesis cause leukemia and disrupt normal hematopoiesis in the zebrafish, providing strong support of the zebrafish as a relevant model system to study mechanisms underlying human leukemia.[18-20] Two distinct waves of zebrafish hematopoiesis have been described. Primitive hematopoiesis is characterized by the generation of embryonic erythrocytes in the intermediate cell mass (ICM)[21] and a distinct population of primitive macrophages that arise from the anterior lateral plate mesoderm (ALPM).[22] Definitive hematopoiesis consists of 2 phases: at first, transient erythromyeloid progenitors (EMPs) form in the posterior blood island (PBI) starting around 24 hours postfertilization (hpf),[23] followed by the appearance of hematopoietic stem cells (HSCs) in the ventral wall of the dorsal aorta by 30 hpf, in a region that is thought to be equivalent to the mammalian aorta-gonad-mesonephros (AGM).[24] These HSCs

then colonize the thymus and the kidney, the hematopoietic organ in adult zebrafish.[24]

We have used the zebrafish model to study the physiologic role of Npm1 and the perturbation in hematopoiesis induced by NPMc+ expression. We identified 2 zebrafish orthologs of the human *NPM1* gene, *npm1a* and *npm1b*, and determined that these genes are required for normal hematopoiesis. Furthermore, we have shown for the first time that *NPMc+* expression causes expansion of primitive and definitive hematopoietic cells in vivo, establishing a platform to further investigate the mechanisms through which NPMc+ contributes to leukemic transformation.

Methods

Zebrafish, microinjections, and WISH

Wild-type AB stocks of *Danio rerio*, the transgenic lines Tg(pu.1: EGFP),[25] Tg(c-myb:EGFP),[26] Tg(cd41:EGFP),[27] Tg(gata1:DsRED),[28] Tg(lmo2:DsRed),[29] and Tg(gata1:EGFP),[30] and the mutant line tp53[zdf1/zdf1] (tp53[M214K/M214K], referred to in the text as p53[m/m])[31] were maintained as described.[32] mRNAs were injected into 1-cell–stage embryos at the indicated amounts. Morpholinos (MOs) targeting the 5′UTR/ATG codon or splice donor sites of *npm1a*, *npm1b*, and control morpholinos, were designed by Gene-Tools LLC. Sequences are given in Table 1. MO concentrations were titrated to the lowest dose resulting in phenotypes: 1.6 ng each for *npm1a* and *npm1b* ATG MOs, 8 ng and 4 ng for *npm1a* splice donor MOs (exon2-intron2(2) and exon3-intron3, respectively), and 4 ng for *npm1b* splice donor MO (exon2-intron2). For experiments in p53-deficient backgrounds, NPM1- or NPMc+–encoding mRNAs were injected into the p53[m/m] line or with the p53 MO (1.6 ng)[33] in the Tg(pu.1:EGFP) line. Observed increases in enhanced green fluorescent protein–positive (EGFP+) cells in the Tg(pu.1:EGFP) line expressing NPMc+ served as an indicator for NPMc+ function.

Developmental staging of injected zebrafish embryos and uninjected controls was determined by somite number. Embryos were fixed in 4% paraformaldehyde (PFA), and assays for mRNA expression using whole-mount in situ hybridization (WISH) were performed as described.[34] Embryos were visualized and imaged with a Nikon SMZ1500 zoom stereomicroscope (Nikon Instruments Inc) using the NIS-Elements software (Nikon Instruments Inc). Some WISH embryos were postfixed in 4% PFA and embedded in 1.5% agar/5% sucrose, equilibrated in 30% sucrose, and cryosectioned (20 μm). All animal protocols were approved by the Dana-Farber Animal Care and Use Committee.

Cloning of human and zebrafish NPM1 cDNAs and RNA production

Full-length NPM1 cDNA (wild-type and mutated) were subcloned in the pCS2+ or p3X-FLAG vector (Sigma) from pGEM-T-easy-NPM1 and

Table 1. MO sequences

Gene	Target	MO sequence
npm1a	ATG/5′UTR	TAATGTTATCCTC**CAT**TTTTGCGCG
npm1a	ATG/5′UTR 5-bp mismatch	TAATcTTATCgTCg**AT**TTTaGCcCG
npm1a	Exon2-intron2 splice donor (2)*	AAGAAACATCACATACCATTCTAAC
npm1a	Exon3-intron3 splice donor	TTATGACCAAGTCTACTTACACTTG
npm1b	ATG/5′ UTR	GACCCATCTGTTCGAGATC**CAT**GTC
npm1b	ATG/5′UTR 5-bp mismatch	GAgCCATgTGTTCGAcATCg**AT**cTC
npm1b	Exon2-intron2 splice donor	TCAAATATTCATCTTCCTCACCGAC
p53	ATG/5′UTR	GCGC**CAT**TGCTTTGCAAGAATTG
Std cont	Human β-globin intron mutation	CCTCTTACCTCAGTTACAATTTATA

Bold letters indicate the ATG codon; lowercase letters, mismatched residues; and Std cont, standard control.

*(2) is the 1 working morpholino of 2 tested (supplemental Figure 1F, available on the *Blood* Web site; see the Supplemental Materials link at the top of the online article).

Table 2. Oligonucleotide sequences

Primer	Sequence
Npm1a forward *Bam*H1	5′-CG**GGATCC**CGCTTCCTGCACTCGTGTTCGCTGAC-3′
Npm1a reverse *Xba*I	5′-GC**TCTAGA**GCGGCCATTCTGAAACCCACTATTC-3′
Npm1b forward *Bam*HI	5′-CG**GGATCC**GCGCAAAATGGAGGATAAC-3′
Npm1b reverse *Xho*I	5′-A**CTCGAG**CGCAGACTTCTGCTGCACT-3′
β-actin forward	5′-CTGGTCGTTGACAACGGCT-3′
β-actin reverse	5′-TCCATCACAATACCAGTAGT-3′

Bold letters indicate restriction enzyme sites.

pGEM-T-easy-NPMmutA.[8] Full-length cDNA encoding EGFP-NPM1 (wild-type and mutated) were subcloned in pCS2+ from pEGFP-C1-NPM1 and pEGFP-C1-NPMmutA.[8] Full-length cDNA of the 2 zebrafish *NPM1* orthologs *npm1a* and *npm1b* were reverse transcription–polymerase chain reaction (RT-PCR)–amplified from 24 hpf AB embryos. Primers for full-length *npm1a* coding region amplification were designed based on the published NCBI sequence (NM_199428), while those for *npm1b* were based on overlapping expressed sequence tag (EST) sequences and the recently annotated Zv8 sequence BC093285 (Table 2). Full-length *npm1a* and *npm1b* amplicons were cloned into pCRII-Topo Dual Promoter vector (Invitrogen), from which WISH probes were made, and then into pCS2+, pEGFP-C1, and pDsRed-Monomer-C1 expression vectors (Clontech). All constructs were verified by sequencing. All mRNAs were transcribed from pCS2+ using the mMessage mMachine kit (Ambion).

Comparative analysis and identification of synteny to human 5q35.1-5q35.2

Genes located in 5q35.1-5q35.2 were identified using the National Center for Biotechnology Information (NCBI) Mapviewer.[35] Zebrafish orthologs for genes in this region were identified using a "reciprocal best-hit" analysis as described.[36] TBLASTN searches were applied for human protein sequences and BLASTX or TBLASTN searches for zebrafish cDNA sequences or proteins, respectively (Ensembl Zv7). Comparative analysis between the human and the 2 zebrafish protein sequences used the Clustal W algorithm.[37]

RT-PCR, protein extraction, WB, and coimmunoprecipitation studies

Total RNA from zebrafish embryos at various stages of development was extracted using Trizol (Invitrogen) following the manufacturer's instructions. RT-PCR was performed on RNA using the Qiagen One-Step RT-PCR Kit using gene-specific primers. Primers used for npm1a and npm1b amplification spanned the full-length coding region. Primers used for β-actin amplification spanned 2 introns. Primer sequences are provided in Table 2. Protein lysates were obtained from single-cell suspensions of approximately 20 zebrafish embryos per condition. Embryos were dissociated with 0.5% trypsin (GIBCO), and protein extraction, Western blot (WB), and coimmunoprecipitation studies were carried out as described.[14] Antibodies used were anti-NPM1, clone 376;[8] anti–β-tubulin (Abcam); anti-GFP (Roche); and anti-FLAG (Sigma).

Fluorescence analysis in zebrafish embryos and 293T cells

For cytospins (Figure 3A-F), 24-hpf embryos injected with EGFP-NPM1 or EGFP-NPMc+ at the indicated doses were dissociated with 0.5% trypsin (GIBCO). The cell suspension was fixed in 4% PFA. A total of 10^5 cells were spun onto glass slides and mounted with ProLong Gold Antifade reagent with DAPI (Molecular Probes). For confocal analysis of EGFP+ cells from whole embryos (Figure 3H-I), 24-hpf embryos injected with EGFP-NPM1 (50 ng) or EGFP-NPMc+ (10 ng) were fixed in 4% PFA, deyolked, and flat-mounted on glass slides with ProLong Gold Antifade reagent with DAPI (Molecular Probes). 293T cells (Figure 4) were seeded on glass coverslips and transfected 24 hours later using Fugene 6 (Roche).

In cotransfection experiments, plasmids were used at equimolar ratios. At 24 hours after transfection, cells were rinsed in phosphate-buffered saline (PBS), fixed in PFA (10 minutes), and mounted on glass slides with ProLong Gold Antifade reagent with DAPI (Molecular Probes). Whole-mount anti–activated caspase-3 and anti-GFP immunostaining (Figure 6) were performed as follows: embryos fixed in 4% PFA were rinsed in PDT (PBST, 0.3% Triton-X, and 1% DMSO), blocked in CAB (10% HI-FBS, 2% BSA in PBST), and incubated with primary antibodies (rabbit anti–activated caspase-3 [BD Biosciences] and mouse anti-GFP [Molecular Probes]) in CAB (1:500). Embryos were then washed in PDT, blocked in CAB, and incubated with secondary antibodies (anti–mouse AlexaFluor-488–conjugated and anti–rabbit AlexaFluor-568–conjugated; Molecular Probes) in CAB (1:200). Acridine orange stains were performed as previously described.[38] Confocal images of 32-hpf Tg(cd41:EGFP), Tg(gata1:dsRed);(c-myb:EGFP), and Tg(lmo2:dsRed);(gata1:EGFP) transgenic embryos injected with NPM1 (50 ng) or NPMc+ (10 ng; Figure 7) were taken from live embryos mounted in 1% low-melting point agarose.

Analysis of zebrafish by flow cytometry

Specific hematopoietic subpopulations from adult dissected kidney marrows were obtained as described.[28] Transgenic embryos were dissociated in liberase blendzyme 3 (Roche) for 30 to 60 minutes at 32°C. Embryos were gently dissociated using a pipette tip, passed through a 40-μM filter, and washed 3 times in cold PBS. Tg(pu.1:EGFP) were labeled with annexin V–phycoerythrin (PE) to assess apoptosis.[38]

DNA content of pu.1:EGFP+ cells was determined by hypotonic propidium iodide (PI) staining of EGFP+ cells sorted on a MoFlo cell sorter (DAKO Cytomation). Fluorescence-activated cell sorter (FACS) analysis of c-myb:EGFP+ cells was conducted in dissected trunks of embryos, gating on the FSC^HIGH population as described in Bertrand et al.[24] Data from Tg(c-myb:EGFP), Tg(pu.1:EGFP), and double Tg(gata1:EGFP);Tg(lmo2:dsRed) cell suspensions were acquired on a FACS-Canto II (BD Biosciences). Dead c-myb:EGFP and pu.1:EGFP cells were excluded by PI staining. Data were analyzed using FlowJo (TreeStar) or Modfit LT (Verity Software).

Results

Identification of 2 zebrafish NPM1 genes

Zebrafish often have 2 copies of genes orthologous to a single mammalian gene as a result of genomic duplication during teleost evolution.[39] To identify the zebrafish npm1 gene(s), the human NPM1 amino acid sequence was used in a TBLASTN search using the Ensembl, University of California Santa Cruz (UCSC), and NCBI platforms. A total of 2 loci were identified, including an annotated zebrafish npm1 gene on chromosome 10 whose protein product exhibits 51% identity to NPM1, and multiple overlapping ESTs encoded by a novel locus on
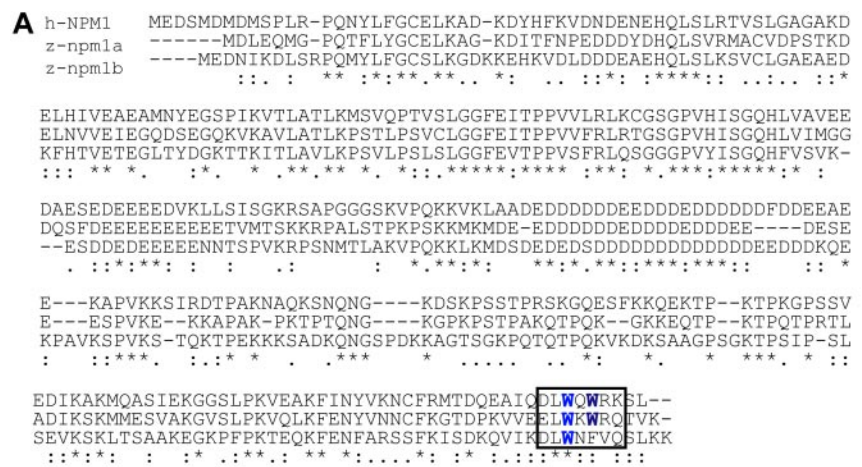
Figure 1. Identification of 2 putative zebrafish npm1 genes. (A) Clustal W alignment of human NPM1 (top row), zebrafish Npm1a (middle row), and Npm1b (bottom row) proteins. * indicates identical residues; colon (:), highly similar residues; and period (.), similar residues. Critical tryptophan residues necessary for nucleolar localization are highlighted in blue in the boxed area. (B) The genomic loci surrounding human NPM1 on chromosome 5q35.1 (top row) are syntenic with the regions where npm1a (on chromosome 10) and npm1b (on chromosome 14) are located in the zebrafish genome (bottom row left and right, respectively). (C) RT-PCRs showing npm1a (top row) and npm1b (middle row) expression levels. β-actin expression levels are used as a loading control (bottom row). Left: npm1a and npm1b embryonic expression was assessed from whole embryos at the indicated time points. Right: RT-PCRs from precursor, lymphoid, myeloid, and erythroid cells sorted from adult kidney marrow (gating strategy based on forward- and side-scatter plots[28]). (D,F,G,I) npm1a or npm1b WISH assays in 24-hpf or 48-hpf embryos, lateral view, anterior to the left, dorsal upwards. (E,H) Close-up dorsal view (anterior to the left) of the brain and anterior trunk in flat-mounted, deyolked 24-hpf embryos stained with npm1a or npm1b probes. Digoxigenin-labeled RNA probes encoding the full-length npm1a and npm1b sequences were transcribed from linearized cDNA constructs using the DIG RNA labeling kit (Roche) following manufacturer instructions.
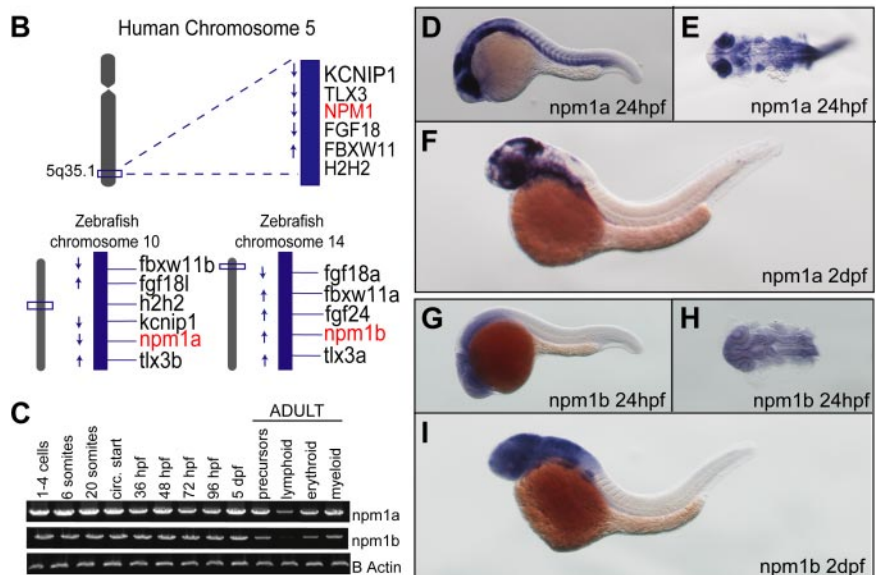
chromosome 14, corresponding to a gene with 48% identity to NPM1 (Figure 1A). In silico analysis of the putative proteins encoded by the 2 genes shows that critical NPM1 functional domains are conserved in both Npm1 zebrafish proteins, including the C-terminal tryptophan residues implicated in nucleolar localization[14] (Figure 1A boxed area; supplemental Figure 1A-B). Furthermore, the genomic regions surrounding both zebrafish *npm1* genes showed high degrees of synteny with human 5q35.1, the locus of human *NPM1* (Figure 1B). Thus, each of these genes is orthologous to NPM1; we refer to these genes as *npm1a* (chromosome 10) and *npm1b* (chromosome 14). Both zebrafish *npm1* genes are expressed maternally and throughout the first 5 days of development (Figure 1C). They are also both expressed in all hematopoietic compartments of the adult kidney marrow (Figure 1C). To investigate the spatial expression pattern of *npm1a* and *npm1b,* we performed WISH and found that both *npm1a* and *npm1b* are ubiquitously expressed at 24 hpf, with highest levels in the developing brain, eye, and somites (Figure 1D-E and 1G-H, respectively). By

2 days after fertilization (dpf), expression was most prominent in the brain and fin-buds (Figure 1F,I).

Knockdown of npm1a and npm1b leads to myeloid cell loss

To determine whether the zebrafish *npm1* genes had a role in hematopoiesis, each gene was knocked down using antisense MOs. Initial studies were carried out using 5′UTR/ATG MOs. Embryos were analyzed for *myeloid peroxidase* (*mpx*) expression by WISH at 2 dpf. Knockdown of each gene individually lead to a significant reduction in the number of *mpx*-expressing cells (Figure 2A,D,G,M). When *npm1a* and *npm1b* were knocked-down simultaneously, the effect on *mpx*-expressing cell numbers was markedly increased (Figure 2J,M). Embryos injected with both MOs together showed developmental abnormalities, with a smaller head and eyes and a shortened yolk extension (Figure 2J; arrow and arrowhead). We further validated the specificity of this phenotype by testing several MOs directed at splice donor sites of *npm1a* and *npm1b*. Combined knockdown of *npm1a* and *npm1b* using the splice donor site MOs
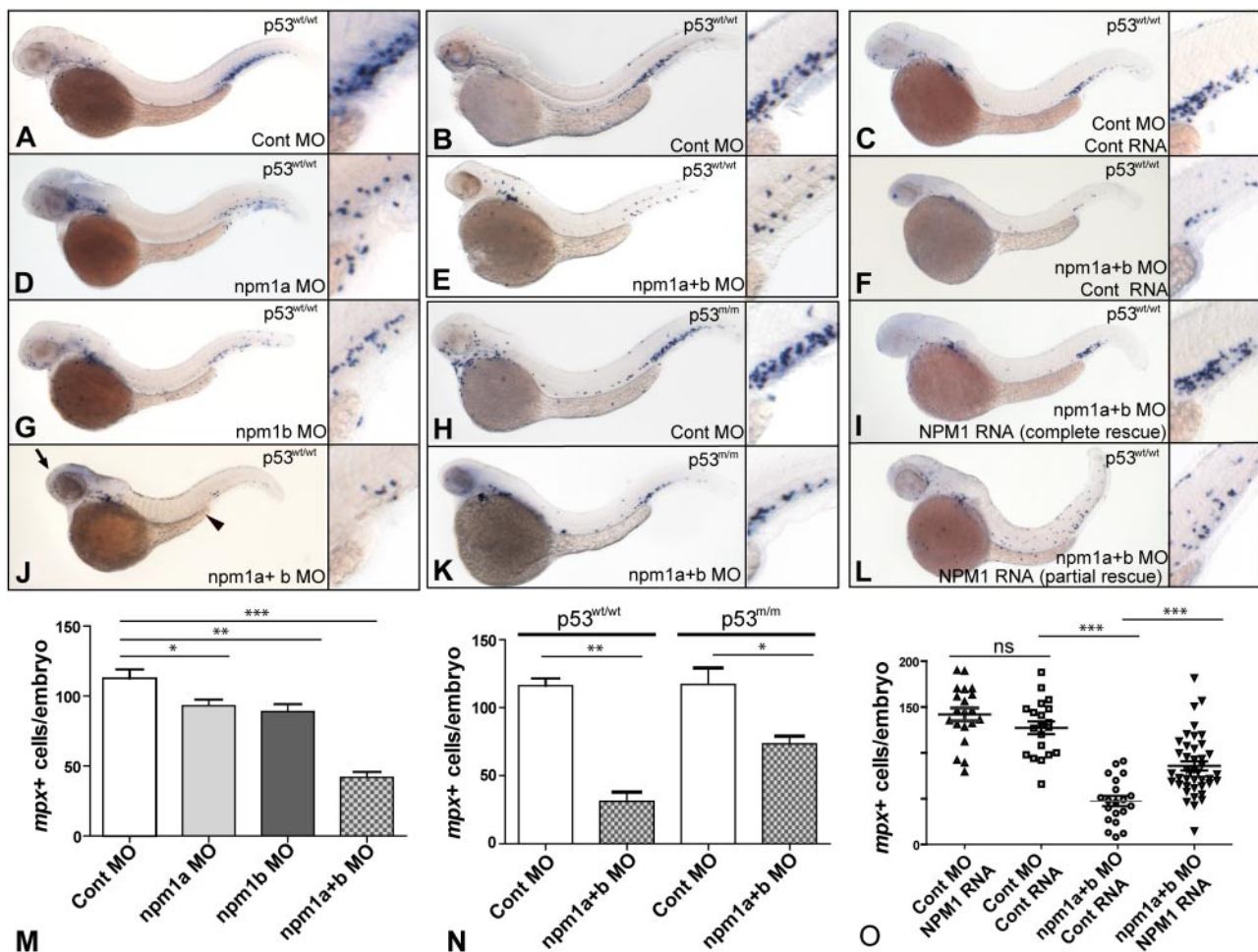
Figure 2. Knockdown of *npm1a* and *npm1b* leads to loss of myeloid cells. (A-L) WISH for *mpx* in 48-hpf embryos, lateral view, anterior to the left, dorsal upwards. (A,D,G,J,M) Knockdown of *npm1* genes results in loss of *mpx*-expressing myeloid cells. A significant difference is seen in myeloid cell numbers when each gene is knocked-down individually (*npm1a* in panel D and *npm1b* in panel G, quantified in panel M); this effect is at least additive in the double knockdown (*npm1a* + *npm1b* in panel J, quantified in panel M). (B,E,H,K,N) *mpx* expression is reduced upon *npm1* knockdown compared with controls in both the p53^wt/wt^ (B,E) and p53^m/m^ (H,K) backgrounds (quantified in panel N). (C,F,I,L,O) Loss of *mpx* expression by knockdown of *npm1* (F) can be rescued completely (I) or partially (L) by NPM1 RNA injection (10 pg). No differential expression of *mpx* is observed when 10 pg NPM1 or 10 pg control RNA (C) are injected with a control MO (quantified in panel O). npm1a MO indicates 5′UTR MO (1.4 ng); npm1b MO, 5′UTR MO (1.4 ng); npm1(a+b), npm1a MO + npm1b MO (1.4 ng each); control MO, npm1a 5-bp mismatch + npm1b 5-bp mismatch at 1.4 ng each. Error bars represent SEM. ns indicates not significant; *$P < .02$; **$P < .01$; ***$P < .001$ (Student t test). Complete rescue in panel I is defined as *mpx*+ cell numbers per embryo greater than the lower limit of the 95% confidence interval of the control RNA/control MO-injected embryos. Partial rescue in panel L is defined as *mpx*+ cells/embryos greater than the upper limit of the 95% confidence interval of the npm1(a+b) MO but below the lower limit of the 95% confidence interval of the control RNA/control MO-injected embryos.

Figure 3. Mutated human NPM1 is aberrantly expressed in the cytoplasm of zebrafish cells. (A-F) Epifluorescence analysis of EGFP-NPM1 (A-C) and EGFP-NPMc+ (D-F) subcellular localization in cytospins of zebrafish cells after mRNA injection at the indicated amounts. NPM1 or NPMc+ proteins are shown in green, and nuclei are counterstained in blue with DAPI. Cells were visualized with a Zeiss Axio imager Z1 microscope using a Zeiss 63×/1.4 numeric aperture (NA) Apochromat oil lens (Carl Zeiss). Images were acquired with Openlab software (Perkin Elmer). (G) WB analysis of protein extracts from NPM1 (top left 3 lanes) and NPMc+ (top right 3 lanes) mRNA-injected embryos. NPM1 expression levels at each mRNA dose are shown along with β-tubulin expression as a loading control (bottom row). The arrows indicate the doses used for subsequent experiments. (H-I) Confocal microscopy of EGFP-NPM1 subcellular localization in zebrafish embryos at 24 hpf injected with 10 pg of EGFP-NPM1 mRNA (H) and 50 pg EGFP-NPMc+ mRNA (I). NPM1 protein is shown in green, while nuclei are counterstained in blue with DAPI. Images of cells were taken in the dorsal trunk region, shown in the insert (H), with a Zeiss LSM 510 META 2-Photon confocal microscope (Carl Zeiss), using a Zeiss 63×/1.4 NA Apochromat oil lens (Carl Zeiss). Images were acquired with the Zeiss LSM 510 software (Carl Zeiss). The EGFP expression patterns shown were representative of cells throughout the embryo.
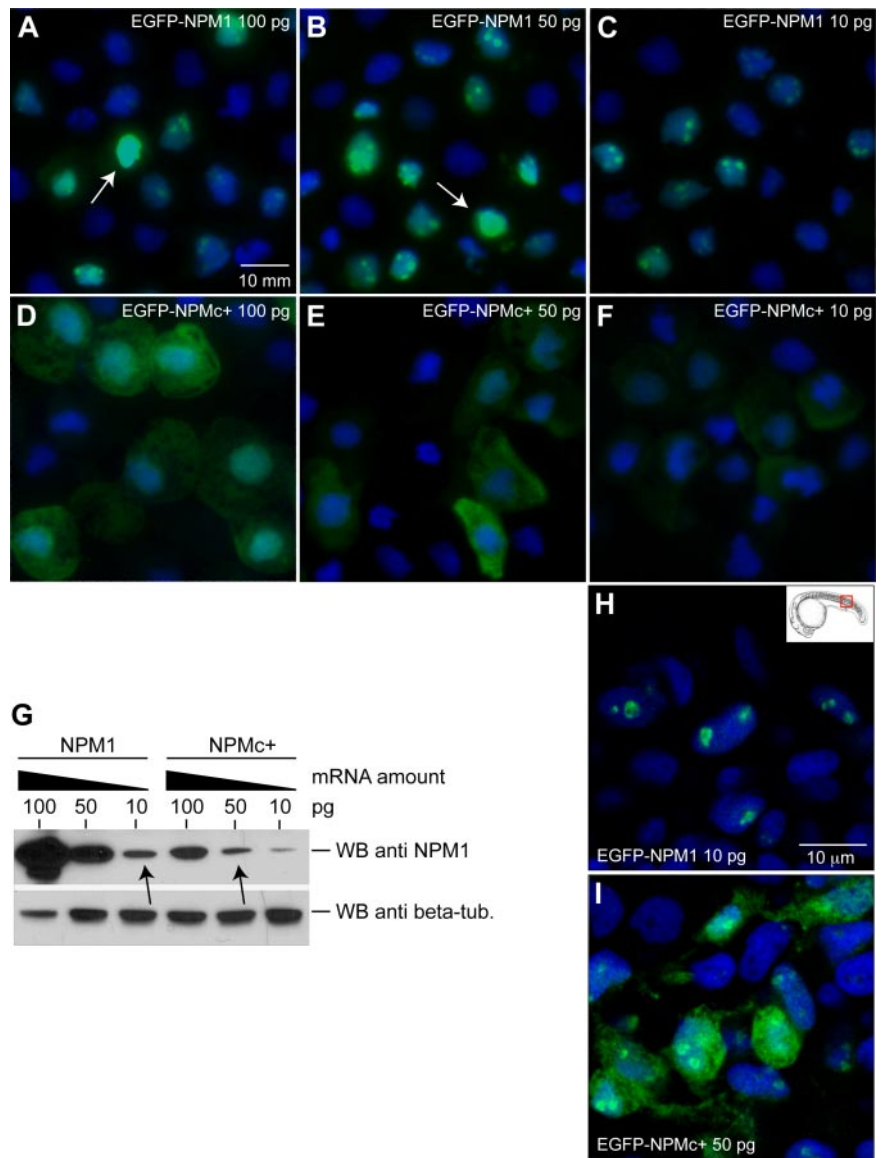
led to the same myeloid phenotype in these morphants as that induced by the 5′UTR/ATG-targeted double morphants (supplemental Figure 1C-D; quantified in supplemental Figure 1E). Knockdown of each gene was confirmed by RT-PCR and sequencing of the products to demonstrate the introduction of a premature stop codon in aberrantly spliced products (supplemental Figure 1F). Because it is known that some MOs can induce p53-dependent cell death as an off-target effect,[40] we knocked-down *npm1a* and *npm1b* in the p53$^{m/m}$ line and analyzed *mpx* expression by WISH at 2 dpf. Compared with control MO-injected p53$^{wt/wt}$ (Figure 2B) and p53$^{m/m}$ (Figure 2H) embryos, injection of *npm1(a+b)* MO in p53$^{m/m}$ embryos led to a significant reduction of *mpx* expression (Figure 2K), similar to that observed in p53$^{wt/wt}$ (Figure 2E; quantifications in Figure 2N). These findings show that the loss of myeloid cells seen after knockdown of *npm1a* and *npm1b* is not a result of p53-dependent MO-induced toxicity.

   To functionally validate *npm1a* and *npm1b* as true orthologs of human *NPM1*, we tested whether NPM1 expression could rescue the *npm1* knockdown phenotype. We injected 1-cell–stage embryos with NPM1 RNA or control (mCherry-encoding) RNA along with *npm1(a+b)* MOs or mismatch controls. Although control RNA injection had no effect in the context of control MO or *npm1(a+b)*

double morphants (Figure 2C,F; quantified in Figure 2O), injection of *NPM1* mRNA (10 pg) rescued both the myeloid and developmental defects when injected into *npm1(a+b)* double morphants. Complete rescue was observed in 15% of embryos (Figure 2I), and a partial rescue was seen in 75% of embryos (Figure 2L). Importantly, NPM1 mRNA injection along with the control MO had no effect on the number of *mpx* cells (quantified in Figure 2O). These results demonstrate that *npm1a* and *npm1b* are true orthologs of *NPM1*.

Mutated human NPM1 is aberrantly expressed in the cytoplasm of zebrafish cells

To test whether NPMc+ was aberrantly localized to the cytoplasm in the zebrafish, as in humans, we injected mRNAs encoding NPMc+ or NPM1 fused to EGFP. The mRNAs were injected into 1-cell–stage embryos at doses up to 100 pg. At the highest dose, embryos appeared normal, and injected and uninjected embryos were morphologically indistinguishable by brightfield microscopic examination at 20 somites. NPM1 protein subcellular localization was assessed using cytospins of cell suspensions obtained from EGFP-NPM1– and EGFP-NPMc+–injected embryos at 24 hpf
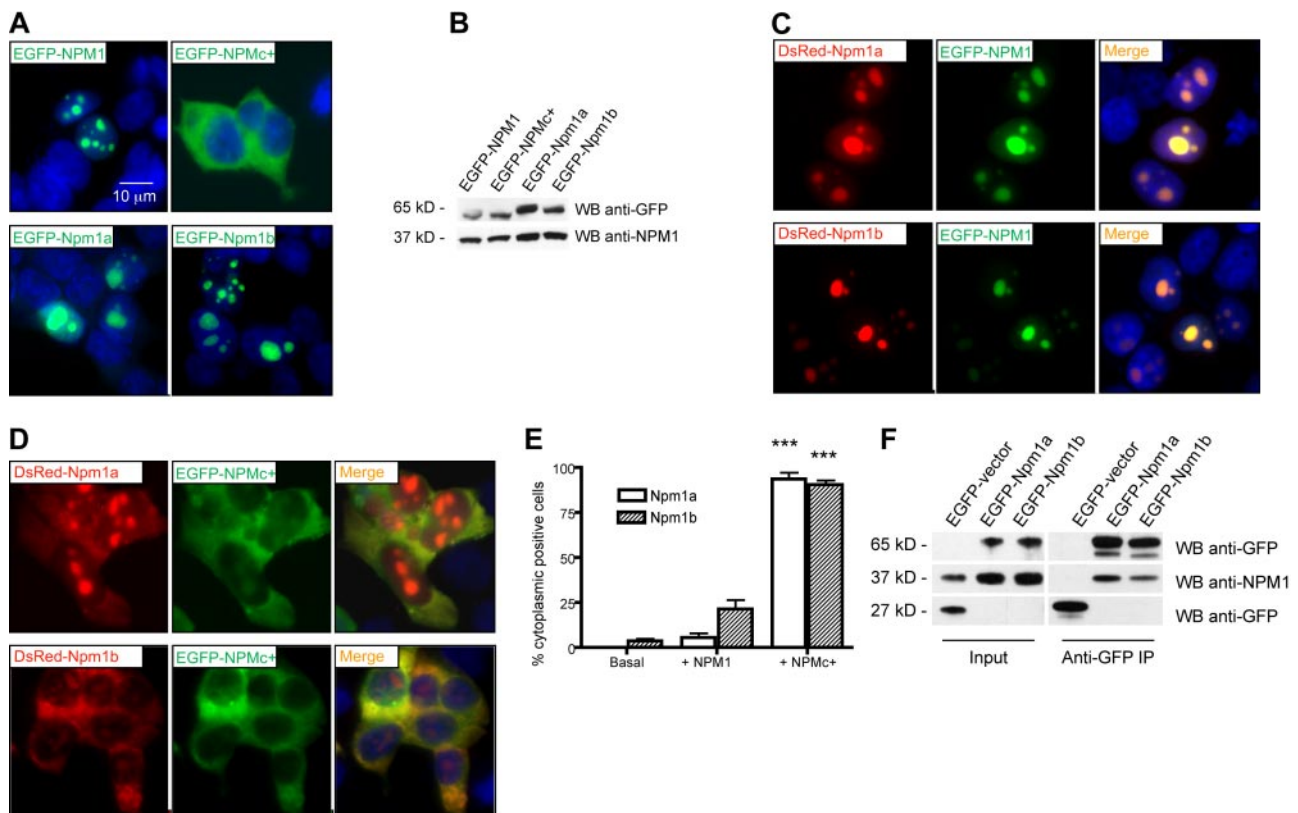
Figure 4. Zebrafish npm1 orthologs interact with human NPM1 protein. (A) Epifluorescent images of 293T cells transfected with pEGFP-C1 expression vector encoding NPM1 (top left), NPMc+ (top right), Npm1a (bottom left), or Npm1b (bottom right). Expressed proteins are shown in green; nuclei are counterstained in blue with DAPI. (B) Anti-GFP WB analysis of protein lysates from transfected cells shown in Figure 2A. Levels of transfected proteins (top row) are shown along with levels of endogenous NPM1 (bottom row). (C) Epifluorescent images of 293T cells cotransfected with pEGFP-C1-NPM1 and pDsRed-monomer-C1 encoding zebrafish Npm1a (top row) or Npm1b (bottom row). Colocalization areas between Npm1a or Npm1b (in red, left column) and NPM1 (in green, middle column) are shown in yellow in the merged images (right column). Nuclei are counterstained in blue with DAPI. (D) Epifluorescent images of 293T cells cotransfected with pEGFP-C1-NPM1c+ and pDsRed-monomer-C1 encoding Npm1a (top row) or Npm1b (bottom row). Colocalization areas between Npm1a or Npm1b (in red, left column) and NPMc+ (in green, middle column) are shown in yellow in the merged images (right column). Nuclei are counterstained in blue with DAPI. All fluorescent images were acquired with a Zeiss Axio imager Z1 microscope using a Zeiss 63×/1.4 NA Apochromat oil lens (Carl Zeiss) and Openlab software (Perkin Elmer). (E) Quantification of the Npm1a and Npm1b delocalization by NPMc+. Bars indicate the percentage of cells with aberrant Npm1a (□) or Npm1b (▨) cytoplasmic expression (with or without residual nucleolar positivity). Error bars indicate SD. *Statistically significant differences between the NPMc+-injected and both NPM1-injected and uninjected embryos (***P < .001; Student t test). More than 200 cells were counted in 3 different microscopic fields for this analysis. (F) Anti-GFP coimmunoprecipitation assays of 293T cells transfected with the empty pEGFP-C1 vector, pEGFP-C1-Npm1a, or pEGFP-C1-Npm1b. Left panels, input; right panels, anti-GFP coimmunoprecipitation lanes. Top row: anti-GFP WB, detecting EGFP-Npm1a and EGFP-Npm1b fusion proteins. Middle row: anti-NPM1 WB, detecting endogenous NPM1. Bottom row: anti-GFP WB, detecting EGFP expressed by the empty vector. In the anti-GFP immunoprecipitation lanes, a dimmer band under the EGFP-Npm1a and EGFP-Npm1b bands probably represents a degradation product of the fusion protein, as it is also visible in the input lanes at longer exposures.

(Figure 3A-F). At low mRNA concentrations (10 pg), EGFP-NPM1 expression was restricted to nucleoli (Figure 3C), while at higher doses (50 and 100 pg), the protein was found to leak into the nucleoplasm and sometimes the cytoplasm of cells (arrows in Figure 3A-B), possibly because of overexpression artifacts. By contrast, NPMc+ was expressed in the cell cytoplasm at all mRNA concentrations (Figure 3D-F), consistent with observations in human NPMc+ AML cases.[8,13] In mammalian cells, NPMc+ cytoplasmic localization is dependent on the presence of a novel nuclear export signal (NES) created by the mutation,[14] and thus this function appears conserved in zebrafish.

We performed WB analysis to determine protein expression levels in lysates from NPM1 or NPMc+ mRNA–injected embryos, and found that wild-type protein levels were much higher than those of NPMc+ at each mRNA dose (Figure 3G). Thus, we selected mRNA doses that yielded comparable protein levels, injecting 10 pg for NPM1 and 50 pg for NPMc+ (2 black arrows in Figure 3G) in all subsequent assays. We validated these selected doses in vivo by analyzing the EGFP-NPM1 and EGFP-NPMc+ protein subcellular localization in embryos by confocal microscopy (Figure 3H-I), confirming the nucleolar restriction of NPM1 and the cytoplasmic distribution of NPMc+ in the vast majority of cells.

Zebrafish NPM1 orthologs interact with human NPM1 proteins

Current evidence supports the hypothesis that the NPMc+ mutant protein heterodimerizes with NPM1 (encoded by the residual normal allele) and may function by shuttling this and other partners out of the nucleus.[13,41] To test whether we could study this mechanism in the zebrafish model, we examined the ability of NPMc+ to interact with zebrafish Npm1 proteins. EGFP- or DsRed-tagged Npm1a and Npm1b were expressed with fluorophore-tagged NPM1 or NPMc+ proteins in human 293T cells to assay for colocalization. First, we confirmed that both EGFP-Npm1a and EGFP-Npm1b were expressed in the nucleoli of cells (Figure 4A bottom left and right, respectively), as was NPM1 (compare with EGFP-NPM1 in Figure 4A top left; and to the cytoplasmic localization of EGFP-NPMc+, top right). WB analysis of transfected cells confirmed that all the proteins were expressed at comparable levels (Figure 4B). When coexpressed with EGFP-NPM1, both DsRed-Npm1a and DsRed-Npm1b colocalized with it in the nucleoli of cells (Figure 4C top and bottom rows, respectively). However, when either Npm1a or Npm1b were coexpressed with EGFP-NPMc+, they became aberrantly expressed in the cytoplasm, with or without residual nucleolar expression, in more than 90% of cells (Figure 4D top and bottom rows, respectively; quantification in Figure 4E). These observations
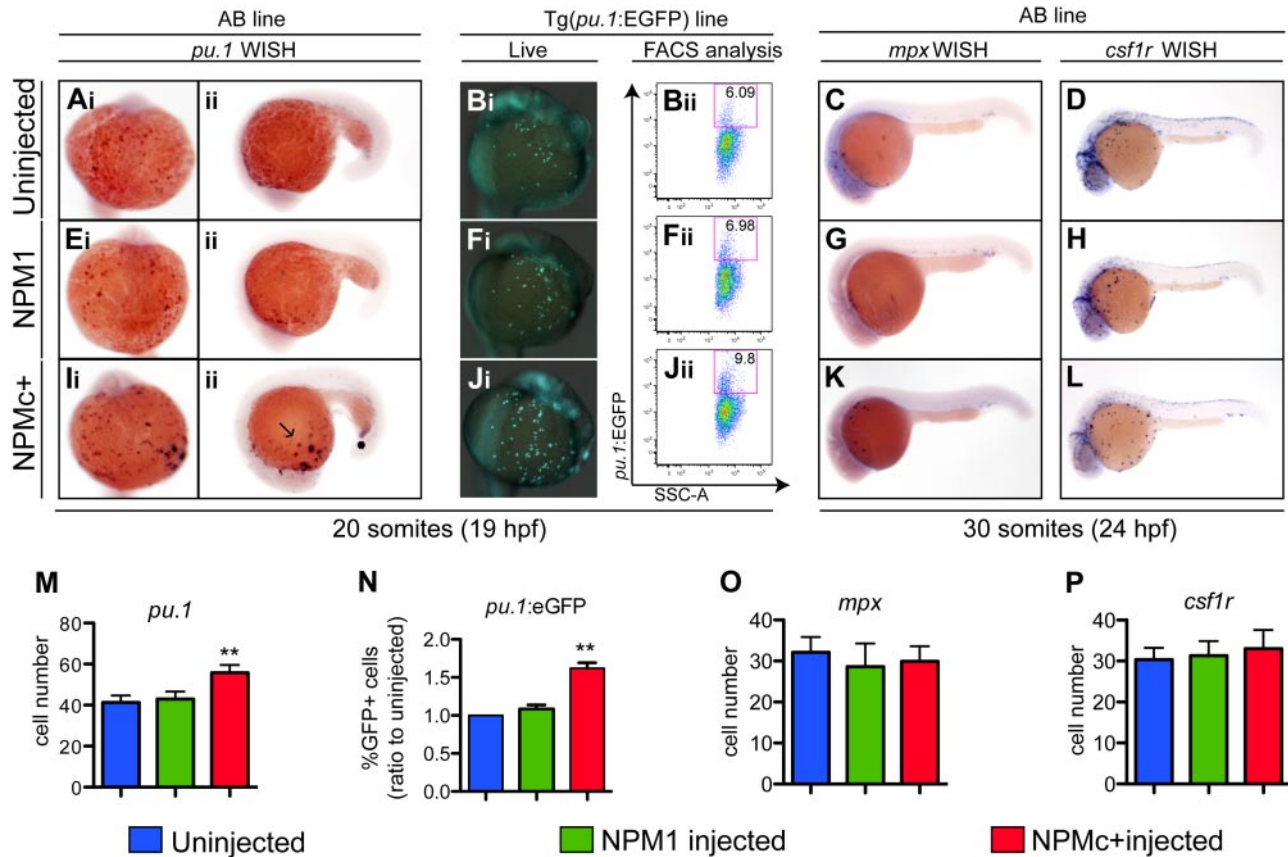
Figure 5. NPMc+ increases the number of primitive myeloid cells in zebrafish embryos. (Ai-Aii,Ei-Eii,Ii-Iii,M) WISH assays of AB embryos showing *pu.1* expression at 20 somites (19 hpf) in ventral views, anterior to the top (A,E,Ii), and lateral views anterior to the left, dorsal upwards (Aii,Eii,Iii). *pu.1*-expressing cells are shown as dark purple dots that increase in number with NPMc+ expression (Ii-Iii). (M) *pu.1+* cell number quantification shows a statistically significant increase upon NPMc+ expression (20 embryos counted per condition). (B,F,J) *pu.1* expression analysis in the Tg(*pu.1*:EGFP) line at 20 somites (19 hpf). Ventral views, anterior to the top, of the ALPM and yolk of live Tg(*pu.1*:EGFP) transgenic zebrafish embryos, uninjected (Bi), or injected with NPM1 10 pg (Fi) or NPMc+ 50 pg (Ji) mRNA. Green cells indicate cells expressing EGFP under the control of the *pu.1* promoter. NPMc+ expression causes a marked increase in EGFP+ cell numbers that disperse widely across the embryo's yolk (Ji). FACS analysis of Tg(*pu.1*:EGFP) embryos, uninjected (Bii), or injected with NPM1 10 pg (Fii) or NPMc+ 50 pg (Jii) mRNA. *EGFP* expression is shown in the y-axis and is increased upon NPMc+ expression (Jii). (N) Quantification of the percentage of EGFP+ cells in 3 independent FACS experiments, each including 50 heterozygous Tg(*pu.1*:EGFP) embryos per condition, normalized to the percentage of EGFP+ cells of uninjected embryos. (C-D, G-H, K-L, O-P) WISH assays showing lateral views (anterior to the left, dorsal upwards) of 30 somites (24 hpf) embryos stained for *mpx* (C,G,K) or *csf1r* expression (D,H,L). No significant change in expression of any of these markers is observed. The number of *mpx* and *csf1r* cells is quantified in panels O and P, respectively (20 embryos counted per condition). Note that the *csf1r* probe also stains xanthophores in the dorsal trunk of the embryo. In all graphs, error bars represent SEM. *Statistically significant differences between the NPMc+-injected and both NPM1-injected and uninjected embryos (**$P < .005$; Student *t* test). In histograms, blue indicates uninjected control embryos; green, NPM1-injected embryos; and red, NPMc+-injected embryos.

indicate that NPMc+ can act in a dominant fashion to redistribute the 2 zebrafish Npm1 proteins to the cytoplasm, similar to human NPM1 (supplemental Figure 2A).[14,41]

To show that human and zebrafish NPM1 proteins can directly bind to each other, we carried out coimmunoprecipitation experiments. Figure 4F shows that an anti-GFP antibody can pull down both EGFP-Npm1a and EGFP-Npm1b along with endogenous NPM1 from transfected 293T cell lysates. In the reciprocal experiment, FLAG-tagged NPM1 and NPMc+ were able to pull down EGFP-tagged Npm1a and Npm1b (supplemental Figure 2B-C). These data demonstrate that NPMc+ can directly interact with zebrafish Npm1 proteins to affect subcellular localization processes, and validates our rationale for testing the consequences of NPMc+ expression in the developing hematopoietic system of zebrafish embryos.

NPMc+ increases the number of primitive myeloid cells in zebrafish embryos

To determine the effects of NPMc+ expression on primitive hematopoiesis, we injected in vitro–transcribed mRNAs encoding NPMc+ (and NPM1 as control) into 1-cell–stage zebrafish embryos, and assayed markers of hematopoietic cell subpopulations

by WISH. We found that expression of NPMc+, but not of NPM1, caused an increase in the number of *pu.1+* cells at 20 somites compared with controls (Figure 5A,E,I; quantified in Figure 5M). These findings were also confirmed by counting *EGFP+* cells in the Tg(*pu.1*:EGFP) transgenic line[25] that expresses EGFP under the control of the *pu.1* promoter (Figures 5Bi,Fi,Ji) and by flow cytometric analysis in the same line (Figures 5Bii,Fii,Jii; quantified in Figure 5N). To determine whether other markers of differentiating early myeloid cells were also expanded, we used probes to detect *mpx* and *csf1r* expression at 30 somites. Surprisingly, we found that neither of these markers was significantly affected by NPMc+ expression compared with NPM1-injected or uninjected embryos (Figure 5C-D,G-H,K-L; quantified in Figure 5O-P).

NPMc+ expression causes an increase in the number of primitive mpx+ and csf1r+ cells in the absence of functional p53

We then asked whether we could see a more marked perturbation of primitive myeloid cell development in the absence of p53. Upon NPMc+ expression *pu.1* cells were increased in the p53[m/m] line at the 20-somite stage to a similar extent as observed in the wild-type background, while NPM1 expression had no effect compared with

uninjected embryos (Figure 6A,E,I; quantified in Figure 6M). Interestingly, we also observed increased numbers of *mpx*- and *csf1r*-expressing cells at the 30-somite stage, providing evidence that a p53-dependent process is required to prevent the increase in *mpx+* and *csf1r+* early myeloid cells induced by NPMc+ (Figure 6C,G,K and Figure 6D,H,L; quantified in Figure 5N-O, respectively). Furthermore, abnormally located *pu.1*- and *mpx*-expressing

cells were also observed in the dorsal trunk and head regions in these fish (Figure 6Iii,K arrows). Additional evidence that NPMc+ perturbs the differentiation of myeloid precursors comes from EGFP+ sorted cells from 30-somite Tg(*pu.1*:EGFP) embryos injected with p53 MO and either NPM1 or NPMc+. Giemsa-stained cytospin slides showed a significant difference in morphology. NPMc+-expressing cells were larger and exhibited more open
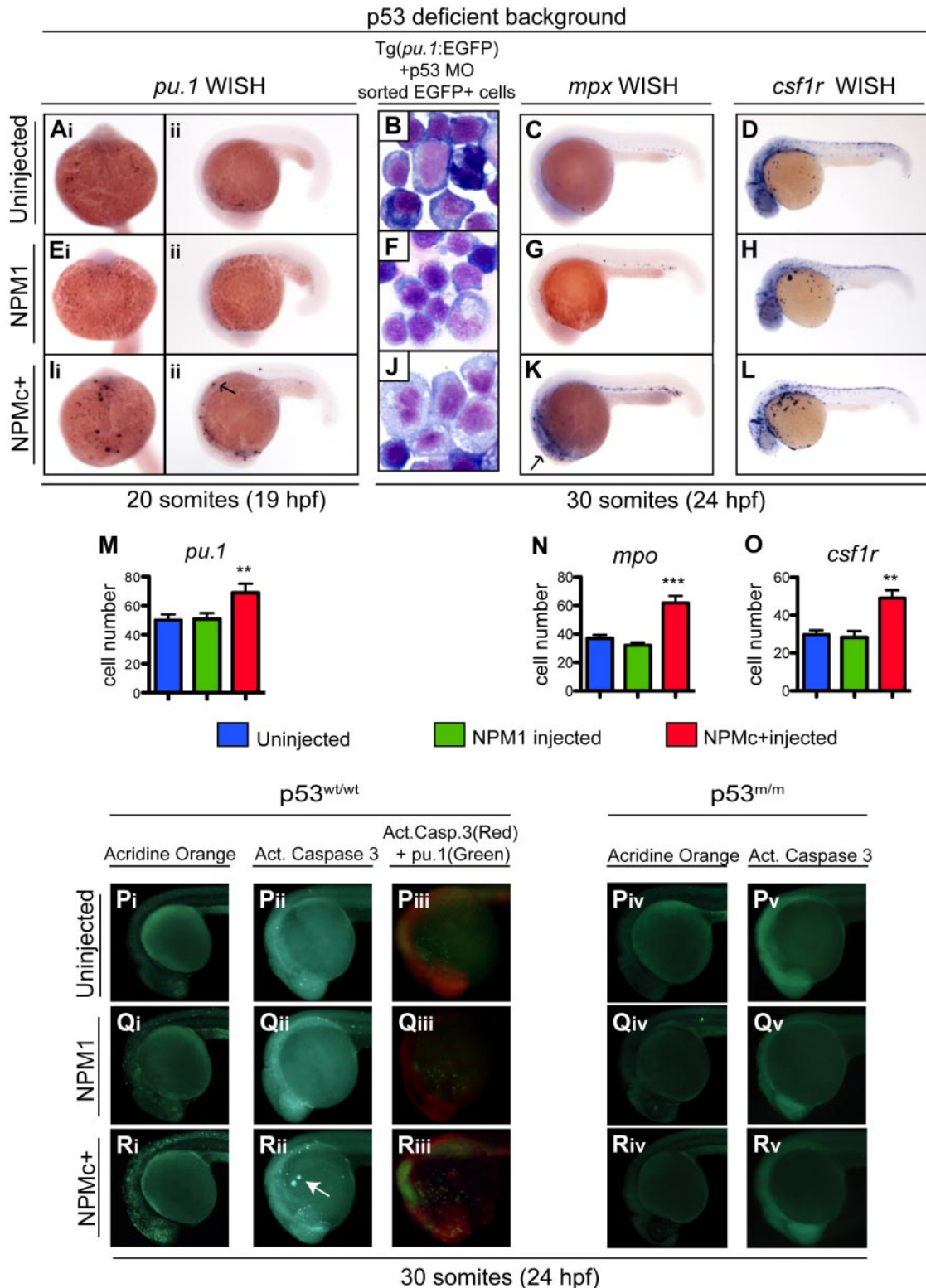
Figure 6.

chromatin, consistent with a more immature phenotype than control and NPM1-expressing cells (Figure 6B,F,J).

## NPMc+ expression causes apoptotic cell death in zebrafish embryos

To determine the mechanism whereby NPMc+ expression resulted in an increase in *pu.1*-expressing early myeloid cells and, later, in *mpx+* and *csf1r+* cells only when p53 was not functional, we used the supravital dye acridine orange to assess cell death due to NPMc+ at 30 somites. NPM1 expression has no effect in hematopoiesis, and therefore served as a control. NPMc+ caused a dramatic increase in cell death detected throughout the embryo, particularly in the eye and brain (Figure 6Ri). In contrast, NPM1-injected embryos (Figure 6Qi) only showed a slight increase in the number of dead cells compared with control uninjected embryos (Figure 6Pi). To further dissect the mechanism of cell death, we also assayed injected embryos for activated caspase-3, which is expressed in apoptotic cells. NPMc+-injected embryos (Figure 6Rii), but not NPM1-injected or uninjected embryos (Figure 6Qii and 6Pii, respectively) showed increased activated caspase-3 staining in the brain and eye, and in cells in the ALPM region (Figure 6Rii arrow). This region corresponds to the location of developing myeloid precursors and suggests that *pu.1+* cells could be undergoing apoptosis. To test this hypothesis, we injected NPM1 or NPMc+ in the Tg(*pu.1:EGFP*) transgenic line, and analyzed embryos for the coexpression of activated caspase-3 (in red) and EGFP (in green). NPMc+-injected embryos showed an increase in both signals compared with uninjected and NPM1-injected embryos (Figure 6Piii,Qiii,Riii); however, colocalization of red and green in the same cell was not detected. These findings were confirmed by FACS annexin-V analysis in Tg(*pu.1*:EGFP) transgenic embryos: NPMc+-injected embryos showed an increase in apoptosis as a whole (supplemental Figure 3A-C) that was not markedly evident in *pu.1:EGFP+* cells (supplemental Figure 3D-F). Furthermore, the cell-cycle profile in sorted EGFP+ cells from Tg(*pu.1*:EGFP) animals showed no difference between control and NPMc+-injected embryos (supplemental Figure 3G-I). Given the marked increase in apoptotic cells evident in NPMc+-injected embryos, we examined the role of p53 in NPMc+-induced cell death. Both wild-type and mutated NPM1 proteins were expressed in the p53[m/m] line, and acridine orange and anti–activated

caspase-3 assays were performed. These assays showed a marked reduction in cell death and apoptosis in p53[m/m] (Figure 6Riv-v, respectively) compared with p53[wt/wt] NPMc+-injected embryos (Figure 6Ri-ii), suggesting that the apoptotic phenotype elicited by NPMc+ is p53-dependent.

NPMc+ increases the number of definitive hematopoietic cells in zebrafish embryos

To investigate whether NPMc+ expression affects definitive hematopoietic cell numbers, we examined the expression of the integrin *cd41* and the transcription factors *c-myb* and *runx1*, which label definitive HSCs starting between 30 and 36 hpf.[24] First, we used Tg(*cd41*:EGFP) transgenic fish to analyze expression of GFP[Low] cells in the AGM region (Figure 7A black box).[24,42] Confocal microscopy showed that NPMc+ expression caused an increase in numbers of *cd41*-EGFP[Low]–expressing cells between the dorsal aorta and the cardinal vein (brackets in Figure 7C,F,I; quantified in Figure 7L), the expected region for developing HSCs, and an increase in EGFP+ cells in the pronephric ducts, ventral to the AGM[24] (arrows in Figure 7C,F,I). Next, we analyzed *c-myb* expression by WISH, and found that NPMc+, but not NPM1, expression causes an increase in the numbers of *c-myb*–expressing cells at 32 hpf (supplemental Figure 4Ai,Ei,Ii; quantified in supplemental Figure 4M). Histologic cross-sections of these embryos confirmed *c-myb*–expressing cells were correctly localized between the ventral wall of the dorsal aorta and the cardinal vein (ie, the AGM region), and NPMc+-injected embryos showed ventral and lateral expansion of these cells within this domain (supplemental Figure 4Aii-iii,Eii-iii,Iii-iii). Importantly, NPMc+ expression caused the same increase in the number of *c-myb*–expressing cells in the AGM of p53[m/m] embryos (supplemental Figure 4D,H,L; quantified in supplemental Figure 4P). Next, we injected NPM constructs into double-transgenic embryos Tg(*c-myb*:EGFP);(*gata1*: DsRED). Z-stack images obtained by confocal microscopy in the AGM region (Figure 7A black box) confirmed that NPMc+ expression increased the number of EGFP+ cells expressed from the *c-myb* promoter relative to controls at 32 hpf (Figure 7Di,Gi,Ji). This observed increase in *c-myb+* cells was confirmed by FACS analysis (supplemental Figure 4B,F,J; quantified in supplemental Figure 4N). As *c-myb* is also expressed in the ICM at this stage,[43] it was important to exclude the possibility that the observed increase

---

Figure 6. NPMc+ expression causes an increase in the number of primitive *mpx+* and *csf1r+* cells in the absence of functional p53 and causes p53-dependent apoptotic cell death. (Ai-Aii, Ei-Eii, Ii-Iii, M) *pu.1* WISH assays in homozygous p53 mutant embryos at 20 somites (19 hpf), uninjected (Ai-Aii), or injected with NPM1 10 pg (Ei-Eii) or NPMc+ 50 pg (Ii-Iii). Embryos are shown in ventral (Ai,Ei,Ii; anterior to the top) and lateral (Aii,Eii,Iii; anterior to the left, dorsal upwards) views. *pu.1*-expressing cells are indicated by dark purple spots and are increased in embryos injected with NPMc+, 50 pg (Ii-Iii). (M) *pu.1+* cell number quantification shows a statistically significant increase upon NPMc+ expression (20 embryos counted per condition). (B,F,J) Giemsa stain of cystospins of *EGFP+* cells sorted from Tg(*pu.1:EGFP*) embryos at 30 somites (24 hpf), injected with p53 MO 1.6 ng alone (B) or in combination with either NPM1 10 pg (F) or NPMc+ 50 pg (J). NPMc+ expression results in larger cells with more immature morphology (J). Images were acquired with a Zeiss Axio imager Z1 microscope using a Zeiss 63×/1.4 NA Apochromat Oil lens (Carl Zeiss) and Openlab software (Perkin Elmer). (C-D, G-H, K-L, N-O) *mpx* (C,G,K) and *csf1r* (D,H,L) WISH are shown in lateral views (anterior to the left, dorsal upwards) of homozygous p53 mutant embryos at 30 somites (24 hpf) uninjected (C-D) or injected with NPM1 10 pg (G-H) or NPMc+ 50 pg (K-L). Note that *mpx* and *csf1r* expression is markedly expanded upon NPMc+ expression and p53 loss (K-L). The number of *mpx* and *csf1r* cells is quantified in panels N and O, respectively (20 embryos counted per condition). Note that the *csf1r* probe also stains xanthophores in the dorsal trunk of the embryo. Error bars represent SEM. *Statistically significant differences between the NPMc+-injected and both NPM1-injected and uninjected embryos (**$P < .005$; ***$P < .001$; Student t test). In histograms, blue indicates uninjected control embryos; green, NPM1-injected embryos; and red, NPMc+-injected embryos. (P-R) Wild-type p53 embryos are shown either uninjected (Pi-Piii), or expressing NPM1 (Qi-Qiii) or NPMc+ (Ri-Riii). All embryos are at 30 somites (24 hpf) and shown in lateral views of the head and anterior trunk, anterior to the left and dorsal upwards. Acridine orange staining (green indicate dead or dying cells) of embryos uninjected (Pi), or injected with NPM1 10 pg (Qi) or NPMc+ 50 pg (Ri) mRNA. An increase in dying cells is observed upon NPMc+ expression (Ri). Activated caspase-3 immunostaining (green indicates cells in apoptosis) of embryos uninjected (Pii), or injected with NPM1 10 pg (Qii) or NPMc+ 50 pg (Rii) mRNA. Increased numbers of apoptotic cells are observed in NPMc+-injected embryos (Rii), forming aggregates on the yolk (arrow). Anti–activated caspase-3 and anti-GFP immunostaining in Tg(*pu.1:EGFP*) transgenic embryos (red spots indicate cells that express the cleaved form of caspase-3, and green spots indicate cells expressing EGFP under the control of the *pu.1* promoter, uninjected (Piii), or injected with NPM1 10 pg (Qiii) or NPMc+ 50 pg (Riii) mRNA. Note in panel Riii the increase in activated caspase-3–expressing cells that surround and lie adjacent to *EGFP+* cells, but do not colocalize with them. Homozygous mutant p53 embryos are shown uninjected (Piv-Pv), or expressing either NPM1 (Qiv-Qv) or NPMc+ (Riv-Rv). All embryos are at 30 somites (24 hpf) shown in lateral views of the head and anterior trunk, anterior to the left and dorsal upwards. Acridine orange staining of embryos uninjected (Piv) or injected with NPM1 10 pg (Qiv) or NPMc+ 50 pg mRNA (Riv) show no difference in the number of dead or dying cells. Anti–activated caspase-3 staining of embryos uninjected (Pv) or injected with either NPM1 10 pg (Qv) or NPMc+ 50 pg mRNA (Rv) show no difference in the number of apoptotic cells. Embryos were equilibrated in glycerol and visualized with a Nikon SMZ1500 zoom stereomicroscope (Nikon) using a 488 nm filter for the EGFP signal and 568 nm filter for the red signal. Images were acquired with NIS-Elements software (Nikon).
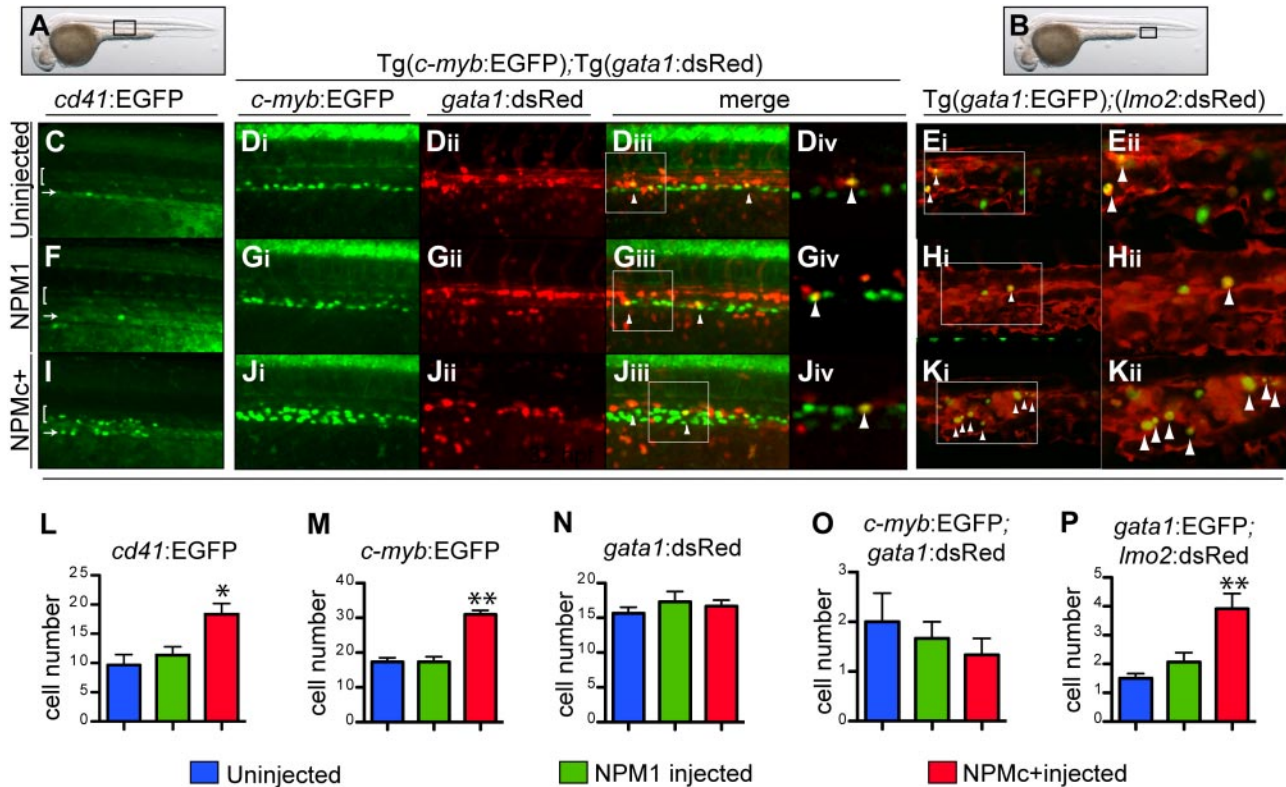
Figure 7. NPMc+ increases the number of definitive hematopoietic cells in zebrafish embryos. (A-B) Brightfield images of a 32-hpf embryo (lateral view, anterior to the left, dorsal upwards) where a black box shows the region of the AGM (A) or of the PBI (B), where subsequent images were taken. (C,F,I,L) Confocal images taken from the AGM region of live 32-hpf Tg(*cd41:EGFP*) transgenic zebrafish embryos (black box in panel A), uninjected (C), or injected with NPM1 10 pg (F) or NPMc+ 50 pg (I) mRNA. Green cells indicate expression of EGFP under the control of the *cd41* promoter. The bracket highlights *cd41*low EGFP+ cells in the AGM region, while the arrow points at the renal EGFP+ population located in the region of the pronephric ducts. EGFP+ cells in the AGM field were counted and showed increased numbers upon NPMc+ expression (L). Images were captured on a Yokogawa spinning disk confocal microscope using a 10×/0.3 NA Plan-fluor phase objective. (Di-iv, Gi-iv, Ji-iv, M-O) Confocal images taken from the AGM region of live 32-hpf Tg(*c-myb*:EGFP);(*gata1*:DsRed) transgenic zebrafish embryos (black box in panel A), uninjected (Di-Div), or injected with NPM1 10 pg (Gi-Giv) or NPMc+ 50 pg (Ji-Jiv) mRNA. Green indicates cells expressing EGFP under the control of the *c-myb* promoter; red indicates cells expressing DsRed under the control of the *gata1* promoter; yellow indicates cells coexpressing both genes (highlighted by arrowheads). The white boxes in panels Diii, Giii, and Jiii indicate an area, magnified in a single Z-stack slice (Div,Giv,Jiv), showing how single slices were used to quantify the number of yellow cells. NPMc+ expression causes an increase in EGFP+ cell numbers in the field of analysis (quantified in panel M) without affecting numbers of cells expressing DsRed under the control of the *gata1* promoter (quantified in panel N) or double-positive cells (quantified in panel O by counting yellow cells in 3 different Z-stack slices in each of 4 embryos). Images were taken as for Tg(*cd41:EGFP*) embryos. (E,H,K,P) Confocal images taken from the PBI region of live 32-hpf Tg(*gata1*:EGFP);(*lmo2*:DsRed) transgenic zebrafish embryos (black box in panel B), uninjected (E), or injected with NPM1 10 pg (H) or NPMc+ 50 pg (K) mRNA. Green indicates cells expressing EGFP under the control of the *gata1* promoter; red indicates cells expressing DsRed under the control of the *lmo2* promoter; yellow indicates cells coexpressing both genes (highlighted by arrowheads). NPMc+ expression causes an increase in cells expressing both genes (K), quantified in panel P by counting yellow cells in 3 different Z-stack slices in each of 4 embryos. Images are single Z-stack slices, and the white boxes in panels Ei, Hi, and Ki indicates an area magnified in panels Eii, Hii, and Kii. Images were acquired on a Yokogawa spinning disk confocal microscope using a 20×/0.75 NA Plan-Apo DIC objective. All confocal images were acquired using the Andor IQ software. Analysis of images was performed using ImageJ software. Error bars represent SEM. *Statistically significant differences between the NPMc+-injected and both NPM1-injected and uninjected embryos (*$P < .05$, **$P < .005$; Student *t* test). In histograms blue indicates uninjected control embryos; green, NPM1-injected embryos; and red, NPMc+-injected embryos.

in *c-myb*–expressing cells did not result from developmentally delayed erythrocytes that can also express *c-myb*. We found that the number of *gata1*:DsRed+ cells was not increased in NPMc+-injected embryos (Figure 7Dii,Gii,Jii; quantified in Figure 7N; also shown by *gata1* WISH; supplemental Figure 5C,F,I). Importantly, we demonstrated that the number of cells coexpressing *c-myb* and *gata1* (yellow cells) was not increased in embryos expressing NPMc+ (arrowheads in Figure 7Diii,Giii,Jiii; magnified single Z-sections showing boxed yellow cells in Figure 7Div,Giv,Jiv; quantified in Figure 7O). Therefore, the increase in *c-myb* was not due to increased numbers of erythroid precursors. To confirm that NPMc+ causes an increase in HSCs in the AGM, we also analyzed *runx1* expression, but surprisingly found that the numbers of *runx1*+ cells were unchanged in NPMc+-injected embryos relative to controls at both the 28- and 32-hpf time points (supplemental Figure 5A-B,D-E,G-H).

We then addressed whether expression of NPMc+ affected the EMP population, which can be identified by gata1/lmo2^BRIGHT

coexpressing cells in the PBI.[23] Confocal microscopic analysis of the PBI region (Figure 7B black box) in double-transgenic Tg(*gata1*:EGFP);(*lmo2*:DsRed) embryos injected with NPMc+ showed a marked increase in numbers of gata1-lmo2 double-positive cells relative to controls (Figure 7E,H,K; quantified in Figure 7P). We confirmed these findings by FACS analysis and found similar increases in the numbers of EMPs upon expression of NPMc+ (supplemental Figure 4C,G,K; quantified in supplemental Figure 4O), again underscoring the finding that NPMc+ perturbs definitive hematopoiesis in the zebrafish embryo.

Discussion

In this report, we have used the zebrafish embryo as a model to examine the role of NPMc+ in hematopoiesis. We identified 2 *npm1* genes orthologous to human *NPM1* and have shown that

loss of both zebrafish *npm1* genes results in a defect in myelopoiesis, which was partially redundant between the 2 genes. This myeloid phenotype is consistent with findings reported in an *Npm1* mouse knockout model,[6] and could be rescued by forced NPM1 expression, indicating functional conservation between human and zebrafish NPM1. Zebrafish embryos injected with human NPMc+–encoding mRNA demonstrated abnormal cellular localization of the mutated protein in the cell cytoplasm, similar to human NPMc+ AML cells, while normal human NPM1 was localized exclusively in the nucleolus. We also demonstrated that both NPM1 and NPMc+ could bind to the zebrafish Npm1 orthologs and regulate their subcellular localization.

We demonstrated that NPMc+ expression perturbs primitive myelopoiesis by examining cells expressing the myeloid markers *pu.1*, *mpx*, and *csf1r*. While *pu.1* is mostly expressed in myeloid precursors at the 20-somite stage,[25] *mpx* is a marker of primitive and definitive granulocytes, and at 30 somites is also expressed in differentiating macrophages.[22] *csf1r* is the zebrafish ortholog of the human macrophage colony-stimulating factor receptor. It is expressed in precursor and mature macrophages on the yolk sac, and in xanthophores of the skin.[44] Interestingly, NPMc+ expression resulted in a striking increase in the number of early *pu.1*-expressing myeloid cells, but only caused a corresponding increase in the numbers of *mpx*- or *csf1r*-expressing myeloid cells later in development in the absence of functional p53. Although our data also showed that NPMc+ expression elicited a generalized p53-dependent apoptotic response, we were unable to demonstrate that the p53-dependent apoptotic cell death was occurring specifically in *pu.1*-expressing myeloid cells upon NPMc+ expression. Technical limitations using reporter zebrafish lines expressing EGFP under the control of the *pu.1* promoter may preclude this analysis, because the EGFP signal is known to be degraded early in the course of apoptosis, and therefore a myeloid apoptotic cell might not simultaneously express both EGFP and cleaved caspase-3 or annexin V. Alternatively, apoptosis could occur within a *pu.1*⁻, *mpx*⁺, and *csf1r*⁺ myeloid cell population at a later stage or a p53-dependent, nonapoptotic cell death process such as senescence could explain these observations. Taken together, these data suggest that NPMc+ expression perturbs primitive hematopoiesis by promoting the early expansion of *pu.1*⁺ myeloid cells, and this phenotype is even more pronounced in a p53-deficient background where *mpx*⁺ and *csf1r*⁺ cells are also expanded. The correlation between p53 mutational status and the extent of the phenotype elicited by NPMc+ is intriguing, because p53 mutations rarely occur in NPMc+ AMLs.[11] However, it has been shown that NPMc+ binds to and inactivates the tumor suppressor p14^{ARF} in mammalian cells, thus inhibiting the p53 response to oncogene activation.[13] Zebrafish and other teleosts lack a homolog of mammalian p14^{ARF},[45] and thus our finding that a p53-dependent apoptotic response is activated by NPMc+ expression may reflect an oncogene-associated cell stress response, which is not evident in human NPMc+ AML cells due to inhibition of p14^{ARF} by NPMc+. These data are also consistent with the myeloproliferative phenotype elicited by NPMc+ expression in a transgenic mouse model,[17] and may be relevant to human AML. Other oncogenes involved in human AML have been shown to disrupt primitive hematopoiesis in zebrafish.[46,47] Moreover, the phenotype induced by the RUNX1:ETO oncoprotein in zebrafish primitive hematopoiesis has been successfully used in a large-scale screen for chemical modifiers,[48] again underscoring the relevance and strengths of the zebrafish system.

Although the transient nature of NPMc+ protein expression after mRNA injection prevents the study of zebrafish hematopoiesis beyond 32 hpf, our data show that definitive hematopoiesis is perturbed by NPMc+, which has important implications for the role of this protein in leukemogenesis. We found that *c-myb*– and *cd41*:EGFP-expressing cells were increased in the ventral wall of the aorta of NPMc+-injected embryos, suggesting that presumptive HSC numbers are increased due to its expression. However, the number of cells expressing *runx1* remains normal at this time. *Runx1* acts upstream of *c-myb* in the development of normal HSCs,[49] suggesting that NPMc+ may expand a *c-myb*⁺/*cd41*⁺ subpopulation of HSCs in which *runx1* expression has already been down-regulated. Alternatively, NPMc+ may specifically down-regulate the expression of *runx1* in these cells. We also showed that NPMc+ expression increases the numbers of *gata1*⁺/*lmo2*^{BRIGHT} double-positive cells in the PBI, indicating expansion of EMPs, the first multipotent, definitive hematopoietic progenitors to develop in both mice and zebrafish. Unlike normal HSCs, EMPs express both *c-myb* and *cd41* but only very low levels of *runx1*, suggesting these could be the main cells targeted by NPMc+ at this time point. However, given the correct anatomical location of *c-myb*-EGFP– and *cd41*-EGFP–expressing cells, we favor the hypothesis that both EMPs and HSCs are expanded by NPMc+. Importantly, it has been recently reported that NPMc+ is expressed in the leukemia-initiating cell fraction of human NPMc+ AMLs.[50,51] In addition, mutated NPMc+ can be found in granulocytic, monocytic, erythroid, and megakaryocytic cells in the bone marrow of patients with NPMc+ AML.[52] These data suggest that a multipotent stem or progenitor cell is the cell of origin for NPMc+ leukemias. Thus, the increase in definitive EMPs and HSCs promoted by NPMc+ expression in zebrafish is likely related to the role of NPMc+ in myeloid leukemogenesis, and provides a tractable in vivo system for study of the mechanisms through which hematopoietic development is perturbed in the presence of NPMc+.

Authorship

Contribution: N.B. and E.M.P. designed and performed research and wrote the manuscript; C.G. contributed important new reagents and analyzed and interpreted data; A.B.J. and J.-S.L. performed research; B.F. designed research and provided important reagents; and J.P.K. and A.T.L. designed research, analyzed data, and wrote the manuscript.

Conflict-of-interest disclosure: B.F. has applied for a patent on the clinical use of NPM1 mutants. The remaining authors declare no competing financial interests.

Correspondence: Niccolò Bolli and A. Thomas Look, Dana-Farber Cancer Institute, Mayer Bldg, Rm M630, 44 Binney St, Boston, MA 02115; e-mail: niccolo_bolli@dfci.harvard.edu, thomas_look@dfci.harvard.edu.

References

1. Grisendi S, Mecucci C, Falini B, Pandolfi PP. Nucleophosmin and cancer. *Nat Rev Cancer.* 2006; 6(7):493-505.

2. Bertwistle D, Sugimoto M, Sherr CJ. Physical and functional interactions of the Arf tumor suppressor protein with nucleophosmin/B23. *Mol Cell Biol.* 2004;24(3):985-996.

3. Korgaonkar C, Hagen J, Tompkins V, et al. Nucleophosmin (B23) targets ARF to nucleoli and inhibits its function. *Mol Cell Biol.* 2005;25(4): 1258-1271.

4. Colombo E, Marine JC, Danovi D, Falini B, Pelicci PG. Nucleophosmin regulates the stability and transcriptional activity of p53. *Nat Cell Biol.* 2002; 4(7):529-533.

5. Wu MH, Yung BY. UV stimulation of nucleophosmin/B23 expression is an immediate-early gene response induced by damaged DNA. *J Biol Chem.* 2002;277(50):48234-48240.

6. Grisendi S, Bernardi R, Rossi M, et al. Role of nucleophosmin in embryonic development and tumorigenesis. *Nature.* 2005;437(7055):147-153.

7. Sportoletti P, Grisendi S, Majid SM, et al. Npm1 is a haploinsufficient suppressor of myeloid and lymphoid malignancies in the mouse. *Blood.* 2008;111(7):3859-3862.

8. Falini B, Mecucci C, Tiacci E, et al. Cytoplasmic nucleophosmin in acute myelogenous leukemia with a normal karyotype. *N Engl J Med.* 2005; 352(3):254-266.

9. Liso A, Bogliolo A, Freschi V, et al. In human genome, generation of a nuclear export signal through duplication appears unique to nucleophosmin (NPM1) mutations and is restricted to AML. *Leukemia.* 2008;22(6):1285-1289.

10. Schlenk RF, Dohner K, Krauter J, et al. Mutations and treatment outcome in cytogenetically normal acute myeloid leukemia. *N Engl J Med.* 2008; 358(18):1909-1918.

11. Falini B, Nicoletti I, Martelli MF, Mecucci C. Acute myeloid leukemia carrying cytoplasmic/mutated nucleophosmin (NPMc+ AML): biologic and clinical features. *Blood.* 2007;109(3):874-885.

12. Arber D, Brunning RD, Le Beau MM, et al. Acute myeloid leukaemia with recurrent genetic abnormalities. In: Swerdlow SH et al, eds. *WHO Classification of Tumours of Haematopoietic and Lymphoid Tissues.* Lyon, France: International Agency for Research on Cancer (IARC). 2008; 110-123.

13. Falini B, Bolli N, Liso A, et al. Altered nucleophosmin transport in acute myeloid leukaemia with mutated NPM1: molecular basis and clinical implications. *Leukemia.* 2009;23:1731-1743.

14. Falini B, Bolli N, Shan J, et al. Both carboxy-terminus NES motif and mutated tryptophan(s) are crucial for aberrant nuclear export of nucleophosmin leukemic mutants in NPMc+ AML. *Blood.* 2006;107(11):4514-4523.

15. Bolli N, Nicoletti I, De Marco MF, et al. Born to be exported: COOH-terminal nuclear export signals of different strength ensure cytoplasmic accumulation of nucleophosmin leukemic mutants. *Cancer Res.* 2007;67(13):6230-6237.

16. Cheng K, Grisendi S, Clohessy JG, et al. The leukemia-associated cytoplasmic nucleophosmin mutant is an oncogene with paradoxical functions: Arf inactivation and induction of cellular senescence. *Oncogene.* 2007;26(53):7391-7400.

17. Cheng K, Sportoletti P, Ito K, et al. The cytoplasmic NPM mutant induces myeloproliferation in a transgenic mouse model. *Blood.* 2010;115(16): 3341-3345.

18. Langenau DM, Traver D, Ferrando AA, et al. Myc-induced T cell leukemia in transgenic zebrafish. *Science.* 2003;299(5608):887-890.

19. Bertrand JY, Traver D. Hematopoietic cell development in the zebrafish embryo. *Curr Opin Hematol.* 2009;16(4):243-248.

20. Payne E, Look T. Zebrafish modelling of leukaemias. *Br J Haematol.* 2009;146(3):247-256.

21. Detrich HW 3rd, Kieran MW, Chan FY, et al. Intraembryonic hematopoietic cell migration during vertebrate development. *Proc Natl Acad Sci U S A.* 1995;92(23):10713-10717.

22. Le Guyader D, Redd MJ, Colucci-Guyon E, et al. Origins and unconventional behavior of neutrophils in developing zebrafish. *Blood.* 2008;111(1): 132-141.

23. Bertrand JY, Kim AD, Violette EP, Stachura DL, Cisson JL, Traver D. Definitive hematopoiesis initiates through a committed erythromyeloid progenitor in the zebrafish embryo. *Development.* 2007;134(23):4147-4156.

24. Bertrand JY, Kim AD, Teng S, Traver D. CD41+ cmyb+ precursors colonize the zebrafish pronephros by a novel migration route to initiate adult hematopoiesis. *Development.* 2008;135(10): 1853-1862.

25. Hsu K, Traver D, Kutok JL, et al. The pu.1 promoter drives myeloid gene expression in zebrafish. *Blood.* 2004;104(5):1291-1297.

26. North TE, Goessling W, Walkley CR, et al. Prostaglandin E2 regulates vertebrate haematopoietic stem cell homeostasis. *Nature.* 2007;447(7147): 1007-1011.

27. Lin HF, Traver D, Zhu H, et al. Analysis of thrombocyte development in CD41-GFP transgenic zebrafish. *Blood.* 2005;106(12):3803-3810.

28. Traver D, Paw BH, Poss KD, Penberthy WT, Lin S, Zon LI. Transplantation and in vivo imaging of multilineage engraftment in zebrafish bloodless mutants. *Nat Immunol.* 2003;4(12):1238-1246.

29. Zhu H, Traver D, Davidson AJ, et al. Regulation of the lmo2 promoter during hematopoietic and vascular development in zebrafish. *Dev Biol.* 2005;281(2):256-269.

30. Long Q, Meng A, Wang H, Jessen JR, Farrell MJ, Lin S. GATA-1 expression pattern can be recapitulated in living transgenic zebrafish using GFP reporter gene. *Development.* 1997;124(20):4105-4111.

31. Berghmans S, Murphey RD, Wienholds E, et al. tp53 mutant zebrafish develop malignant peripheral nerve sheath tumors. *Proc Natl Acad Sci U S A.* 2005;102(2):407-412.

32. Westerfield M. The zebrafish book: a guide for the laboratory use of zebrafish (*Danio rerio*). 4th edition. Eugene, OR: University of Oregon Press, 2000.

33. Langheinrich U, Hennen E, Stott G, Vacun G. Zebrafish as a model organism for the identification and characterization of drugs and genes affecting p53 signaling. *Curr Biol.* 2002;12(23):2023-2028.

34. Bennett CM, Kanki JP, Rhodes J, et al. Myelopoiesis in the zebrafish, *Danio rerio. Blood.* 2001; 98(3):643-651.

35. National Center for Biotechnology Information (NCBI). Mapviewer. Available at: http://www.ncbi.nlm.nih.gov.ezp-prod1.hul.harvard.edu/mapview/. Accessed August 2006.

36. Barbazuk WB, Korf I, Kadavi C, et al. The syntenic relationship of the zebrafish and human genomes. *Genome Res.* 2000;10(9):1351-1358.

37. European Informatics Institute. Clustal W algorithm. Available at: http://www.ebi.ac.uk/Tools/clustalw2/index.html. Accessed January 2009.

38. Sidi S, Sanda T, Kennedy RD, et al. Chk1 suppresses a caspase-2 apoptotic response to DNA damage that bypasses p53, Bcl-2, and caspase-3. *Cell.* 2008;133(5):864-877.

39. Gates MA, Kim L, Egan ES, et al. A genetic linkage map for zebrafish: comparative analysis and localization of genes and expressed sequences. *Genome Res.* 1999;9(4):334-347.

40. Robu ME, Larson JD, Nasevicius A, et al. p53 activation by knockdown technologies. *PLoS Genet.* 2007;3(5):e78.

41. Bolli N, De Marco MF, Martelli MP, et al. A dose-dependent tug of war involving the NPM1 leukaemic mutant, nucleophosmin, and ARF. *Leukemia.* 2009;23(3):501-509.

42. Kissa K, Murayama E, Zapata A, et al. Live imaging of emerging hematopoietic stem cells and early thymus colonization. *Blood.* 2008;111(3): 1147-1156.

43. Thompson MA, Ransom DG, Pratt SJ, et al. The cloche and spadetail genes differentially affect hematopoiesis and vasculogenesis. *Dev Biol.* 1998;197(2):248-269.

44. Hall C, Flores MV, Storm T, Crosier K, Crosier P. The zebrafish lysozyme C promoter drives myeloid-specific expression in transgenic fish. *BMC Dev Biol.* 2007;7:42.

45. Gilley J, Fried M. One INK4 gene and no ARF at the Fugu equivalent of the human INK4A/ARF/INK4B tumour suppressor locus. *Oncogene.* 2001;20(50):7447-7452.

46. Kalev-Zylinska ML, Horsfield JA, Flores MV, et al. Runx1 is required for zebrafish blood and vessel development and expression of a human RUNX1-CBF2T1 transgene advances a model for studies of leukemogenesis. *Development.* 2002;129(8):2015-2030.

47. Liu TX, Rhodes J, Deng M, et al. Dominant-interfering C/EBPalpha stimulates primitive erythropoiesis in zebrafish. *Exp Hematol.* 2007;35(2): 230-239.

48. Yeh JR, Munson KM, Elagib KE, Goldfarb AN, Sweetser DA, Peterson RT. Discovering chemical modifiers of oncogene-regulated hematopoietic differentiation. *Nat Chem Biol.* 2009;5(4):236-243.

49. Burns CE, Galloway JL, Smith AC, et al. A genetic screen in zebrafish defines a hierarchical network of pathways required for hematopoietic stem cell emergence. *Blood.* 2009;113(23):5776-5782.

50. Martelli MP, Pettirossi V, Bonifacio E, et al. Evidence for CD34+ hematopoietic progenitor cell involvement in acute myeloid leukemia with NPM1 gene mutation: implications for the cell of origin [abstract]. *Blood.* 2008;112(11):Abstract 307.

51. Taussig DC, Vargaftig J, Miraki-Moud F, et al. Leukemia initiating cells from some acute myeloid leukemia patients with mutated nucleophosmin reside in the CD34- fraction. *Blood.* 2010;115(10): 1976-1984.

52. Pasqualucci L, Liso A, Martelli MP, et al. Mutated nucleophosmin detects clonal multilineage involvement in acute myeloid leukemia: Impact on WHO classification. *Blood.* 2006;108(13):4146-4155.